Anchorage-dependent multicellular aggregate formation induces CD44 high cancer stem cell-like ATL cells in an NF-κB- and vimentin-dependent manner

Yukiko Miyatake,[1, 2] Noreen Sheehy,[2] Shunji Ikeshita,[1]

William W. Hall,[2] and Masanori Kasahara[1]

[1]Department of Pathology, Hokkaido University Graduate School of Medicine, Sapporo 060-8638, Japan; and [2]Centre for Research in Infectious Diseases, School of Medicine and Medical Science, University College Dublin, Dublin 4, Ireland

Running title: **Expansion of CD44 high CSC-like ATL cells**

Word counts: 3224 ; Number of figures: 6; Reference counts: 47

Key words; cancer stem cells, coculture, CD44, vimentin, ATL

Correspondence: Dr. Yukiko Miyatake,

Department of Pathology, Hokkaido University Graduate School of Medicine, Kita-15, Nishi-7, Kita-ku, Sapporo 060-8638, Japan

Phone: +81-11-706-5050;

Fax: +81-11-706-7825; E-mail: yukimiya@med.hokudai.ac.jp

ABSTRACT

Adult T-cell leukemia/lymphoma (ATL) is an intractable T-cell malignancy accompanied by massive invasion of lymphoma cells into various tissues. We demonstrate here that ATL cells cultured on a layer of epithelial-like feeder cells form anchorage-dependent multicellular aggregates (Ad-MCAs) and that a fraction of MCA-forming ATL cells acquire CD44 high cancer stem cell-like phenotypes. ATL cells forming Ad-MCAs displayed extracellular microvesicles with enhanced expression of CD44v9 at cell synapses, augmented expression of multidrug resistance protein 1, and increased NF-κB activity. Blockade of the NF-κB pathway dramatically reduced Ad-MCA formation by ATL cells and the emergence of CD44 high ATL cells, but left a considerable number of ATL cells adhering to the feeder layer. Disruption of vimentin cytoskeleton by treatment with withaferin A, a natural steroidal lactone, suppressed not only the adhesion of ATL cells to the feeder layer but also subsequent Ad-MCA formation by ATL cells, suggesting the involvement of vimentin in anchoring ATL cells to the feeder layer. Ad-MCA formation by ATL cells on a layer of epithelial-like feeder cells may mimic critical events that occur in metastatic colonization.

1. INTRODUCTION

Adult T-cell leukemia/lymphoma (ATL) is an intractable and fatal T-cell malignancy caused by human T-cell leukemia virus type 1 (HTLV-1) [1]. A striking feature of ATL is a massive invasion of lymphoma cells into various tissues such as the gastrointestinal tract, lung, skin, and central nervous system [2, 3]. Leukemia/lymphoma cells that have invaded the tissues become more resistant to chemotherapy, presenting a major obstacle to the treatment of ATL patients [4-6]. However, the mechanisms underlying the acquisition of intractable phenotypes by tissue-invading ATL cells are largely unknown.

Cancer stem cells (CSCs) are defined as a small fraction of tumor cells that display properties of self-renewal, high tumorigenicity, and drug resistance, resulting in cancer metastasis and recurrence [7, 8]. Of many CSC markers identified thus far, CD44 is of particular biologic importance [9]. Recent work has revealed that nuclear CD44 directly reprograms stem cell properties in colon cancer cells [10]. Also, expression of CD44 splice variants containing exons 8-10 (CD44v8-10) contributes to reactive oxygen species (ROS) defense by up-regulating the synthesis of a major antioxidant, glutathione [11]. In ATL patients, CD44 is expressed on skin-infiltrating tumor cells, with the plasma levels of soluble CD44 showing correlation with disease severity [12], suggesting the existence of $CD44^+$ ATL stem cells. Cancer cells with constitutively

activated NF-κB tend to become resistant to various anticancer drugs and radiotherapy [13, 14], suggesting a close link between CSC phenotypes and NF-κB activation [15, 16]. Notably, constitutive activation of NF-κB is observed in ATL cells, despite the fact that they do not express detectable levels of viral gene products such as Tax with potent NF-κB-activating activities [17, 18].

CSC properties are thought to be regulated and maintained by the surrounding microenvironment (niche) composed of cellular structures such as epithelium, vasculature, mesenchymal cells and extracellular matrix [19-21]. However, the mechanisms of how CSCs emerge and are maintained in the niche are poorly understood mainly because of the difficulty in expanding CSCs *in vitro*. Feeder cells have been used to support the growth and stemness potential of stem cells *in vitro* [22-25]. Mesenchymal cells such as mouse embryonic fibroblasts and human mesenchymal stem cells have been successfully employed as feeder cells to support the growth of human embryonic and induced pluripotent stem cells [23-25]. Although human embryonic cells can be maintained under feeder-free conditions, absence of feeder cells often results in karyotype abnormalities due to chromosomal instability [26, 27]. Given the basic similarities of CSCs and normal stem cells, it is reasonable to assume that feeder cells play a similarly important role in the emergence of CSCs and

the formation of CSC niches.

We previously showed that ATL cells undergo apoptosis when cultured in the presence of histone deacetylase (HDAC) inhibitors; however, when ATL cells were directly cocultured with HEK293T cells, a normal tissue-derived epithelial-like cell line, they acquired resistance to HDAC-inhibitor-induced apoptosis [28]. Interestingly, the majority of ATL cells adhering to HEK293T cells became quiescent and slowed down cell cycle progression, and some ATL cells acquired CD44 high phenotypes. The present study was undertaken to investigate the nature of CD44 high ATL cells induced by simple coculture with HEK293T cells and to study the mechanism by which coculture induces such ATL cells.

2. MATERIALS AND METHODS

2.1. Cells. ATL-CR and ATL-TH, both IL-2-independent ATL cell lines in which HTLV-1 gene expression was silenced [28], were maintained in RPMI-1640 medium supplemented with 10% fetal bovine serum (FBS) and penicillin/streptomycin. HEK293T cells, human embryo kidney-derived epithelial-like cells used as normal tissue-derived feeder cells, were maintained in Dulbecco's minimal essential medium (DMEM) supplemented with 10% FBS and penicillin/streptomycin. 1C3IKEI, a primary normal human embryonic pancreas-derived epithelial-like cell line, was purchased from the RIKEN Bio-Resource center (Tsukuba, Japan) and maintained in DMEM supplemented with 15% FBS. Jurkat, a $CD44^{-}$ T-cell lymphoma cell line, and HuT-78, a T-cell lymphoma line derived from a patient with Sezary syndrome [29], were used as $HTLV\text{-}1^{-}$ T-cell lymphoma cells. ATL-CR, ATL-TH, Jurkat, and HuT-78 were maintained in RPMI-1640 medium supplemented with 10% FBS and penicillin/streptomycin. Fresh ATL cells were obtained from an ATL patient with acute type after written informed consent. This patient had a white blood cell count of 29,520/μl, of which 88% were lymphocytes. Peripheral blood mononuclear cells (PBMCs) were isolated from heparinized peripheral blood by Ficoll-Paque^{TM} PLUS (GE Healthcare Life Sciences, Little Chalfont, UK) and stocked at -148°C immediately.

The experiments involving human blood samples were approved by the Medical Ethics Committee of Hokkaido University Graduate School of Medicine.

2.2. Antibodies (Abs), plasmids, and reagents. Rat monoclonal Ab (mAb) for CD44 (IM7, eBioscience, San Diego, CA), mouse mAb for human vimentin (V9, DAKO Glostrup, Denmark), rat mAb for human CD44v9 (clone RV3; CosmoBio, Tokyo, Japan), and mouse mAb for human multidrug resistance protein 1 (MDR1), also known as P-glycoprotein (UIC2, eBioscience), were used for immunofluorescence staining. Rabbit anti-Nanog (D73G4 XP) and rabbit anti-Sox2 (D6D9 XP) mAbs were purchased from Cell Signaling Technology (Beverly, MA). Mouse anti-HTLV-1 Tax mAb (1A3; Abcam, Cambridge, UK) was used for western blotting. NF-κB activation was measured using pNF-κB-Luc (Stratagene, Santa Clara, CA). HDAC inhibitors such as trichostatin A (TSA), valproic acid sodium salt (VPA), and sodium butyrate (NaB) were purchased from Sigma-Aldrich (St. Louis, MO). Bay 11-7082 (Sigma-Aldrich) [17], an NF-κB inhibitor, was stored as a 100 mM stock in DMSO at 4°C. Withaferin A (WFA) [30], a natural steroidal lactone, was purchased from Merck (Darmstadt, Germany).

2.3. Coculture. ATL cells (5×10^5) were cocultured overnight with HEK293T cells

using the direct coculture system that allowed for cell-cell contact. ATL cells were added to HEK293T cells which had been precultured overnight and formed a monolayer in a 24-well plate. In some experiments, ATL cells or feeder cells were labeled with 1 μM of 5- (and 6-) carboxyfluorescein diacetate succinimidyl ester (CFSE) at a concentration of 1×10^6 cells/ml in PBS for 20 min at 37°C and then washed 3 times in PBS. CFSE-labeled cells were used immediately for each experiment.

2.4. Immunofluorescence staining. This was performed as previously described [31]. In brief, cells cultured on chamber slides were fixed with 4% paraformaldehyde for 15 min. For intracellular staining, cells were treated with PBS containing 0.1% Triton X-100 for 4 min and then fixed with ice-cold 70% methanol for 4 min. Nonspecific binding was blocked with PBT (0.05% Tween-20 in PBS) containing 0.1% goat serum for 10 min. After incubation with primary Ab for each targeted protein, Alexa Fluor-conjugated goat polyclonal Ab was used as a secondary Ab. Throughout this study, an upright fluorescence microscope was used for the observation of stained cells. Images were acquired using an Olympus DP70 camera with its own DP controller software (Olympus, Tokyo, Japan). The ImageJ 1.46 software package [32] was used for image analysis.

2.5. Flow Cytometry (FCM) analysis. Cell cycle distribution of ATL cells was analyzed by DNA content using the propidium iodide staining method as previously described [28].

2.6. Functional assays. Reporter genes were introduced into ATL cells directly using Fugene transfection reagents (Roche Diagnostics, Branchburg, NJ) according to the manufacturer's instructions. ATL-CR cells (5×10^5) were cultured in 60-mm dishes and cotransfected with 1 μg of NF-κB firefly luciferase reporter plasmids together with 50 ng of the *Renilla* luciferase reporter pRL-TK. At 18 h after transfection, ATL-CR cells were washed 5 times in PBS and then cocultured with HEK293T cells in the presence of TSA in triplicate in 24-well plates (2×10^5 cells/well). Reporter activities were measured using the Dual Luciferase reporter assay system (Promega, San Luis Obispo, CA). Reporter activities were normalized using *Renilla* luciferase values.

3. RESULTS

3.1. Anchorage-dependent multicellular aggregate (Ad-MCA) formation induces a population of CD44 high ATL cells

To induce mass formation by ATL cells, we cocultured ATL cells directly with HEK293T cells (Figure 1A). When ATL cells were cocultured overnight on a monolayer of HEK293T cells, the majority of ATL cells adhered to and formed masses on the monolayer, but coculture with normal-tissue-derived fibroblasts failed to induce such mass formation by ATL cells [28]. To determine whether mass formation by ATL cells was induced by clonal proliferation or cellular aggregation of ATL cells, we cocultured a mixture of CFSE- or CytoRed-labeled ATL-CR cells with HEK293T cells (Figure 1B, left panel). After overnight coculture, cell masses composed of a mixture of green- and red-fluorescent cells were observed on the feeder layer, indicating that ATL cells formed multicellular aggregates (MCA) in an anchorage-dependent manner (Figure 1B, right panels).

Next, we examined whether CD44 high ATL cells can be induced by coculture on the feeder layer. HEK293T cells showed neither mRNA expression (data not shown) nor positive staining for CD44 (Figure 1C). The percentage of cell surface $CD44^{+}$ cells as assessed by FCM was 30.8% in ATL-CR cells cultured alone (data not shown), but

only less than 2% of ATL-CR cells expressed CD44 at high levels both on the cell surface and in the cytoplasm when assessed by immunohistochemistry (Figure 1D, upper panel arrowheads). In contrast, when ATL-CR cells were cocultured on a monolayer of HEK293T cells, the proportion of CD44 high ATL cells was increased markedly (Figure 1D, lower panel). Staining for CD44 was more pronounced in ATL-CR cells located at the upper and middle portions of MCAs, whereas vimentin expression was enhanced at the lower portion of MCAs close to the monolayer of HEK293T cells (Figures 1D, lower panels). Similar MCA formation was observed when ATL-TH cells (data not shown), PBMCs from an acute-type ATL patient (Figure 1E), and HuT-78 Sezary cells were cultured on a monolayer of HEK293T cells (Figure 1F).

Interestingly, ATL cells in the upper portion of MCAs were strongly positive for CD44, adhered to each other tightly, and exhibited $CD44^{+}$ extracellular microvesicles at cell-cell junctions (Figure 2A, arrowheads on the left panels). Similar microvesicles were observed in Hut-78 cells forming Ad-MCAs on a feeder layer (Figure 2B). Higher magnification images of MCA-forming ATL cells revealed $CD44v9^{+}$ extracellular microvesicles at cell-cell junctions (Figure 2A, right panels).

3.2. Some MCA-forming CD44 high ATL cells express pluripotency markers

Recent evidence indicates that nuclear CD44 directly reprograms stem cell properties [10]. Nanog is a key transcription factor regulating cellular pluripotency in embryonic stem cells and CSCs [33], and interacts with CD44 directly [14]. Therefore, we examined whether CD44 high ATL cells forming Ad-MCAs express Nanog. After overnight coculture with HEK293T cells, $Nanog^{+}$ cells were frequently observed in Ad-MCA-forming cells, and some of them clearly coexpressed CD44 (Figure 2C). ATL cells located at the upper and middle portions of MCAs tended to exhibit colocalization of CD44 and Nanog signals (Figure 2C, arrowheads). Quantitatively, approximately one third of MCA-forming ATL-CR cells expressed CD44, of which ~8% coexpressed Sox2 (Figure 2D). Notably, Nanog and Sox2 signals were also detected in $CD44^{-}$ ATL cells adhering to CD44 high ATL cells (Figures 2C and D, arrows). Approximately 6% of $CD44^{-}$ MCA-forming ATL-CR cells expressed Sox2 (Figure 2D). These cells were surrounded by CD44 high, $Sox2^{-}$ ATL cells (Figure 2D, left panels). In contrast, pluripotency marker-positive cells were virtually absent in non-MCA-forming ATL cells (data not shown). $Nanog^{+}$ CD44 high ATL cells also emerged in MCA-forming ATL cells when PBMCs isolated from an acute-type ATL patient were cultured on a layer of HEK293T cells (data not shown). These results indicate that Ad-MCA formation induces a population of CSC-like, CD44 high ATL cells expressing pluripotent stem cell

markers.

3.3. ATL cells forming Ad-MCAs augment MDR1 expression

ATL cells undergo apoptosis when cultured alone in the presence of HDAC inhibitors. However, they become resistant to HDAC-inhibitor-induced apoptosis when cocultured with HEK293T cells [28]. We therefore examined whether MDR1 expression is increased in MCA-forming ATL cells. We confirmed that MCA formation makes ATL-CR cells resistant to TSA-induced apoptosis and increases a proportion of cells at G0/G1 phase (Figure 3A). We also confirmed by western blotting that TSA treatment for 24 h did not induce expression of HTLV-1 Tax in ATL-CR cells cultured alone (data not shown). FCM analysis showed increased cell-surface expression of MDR1 on MCA-forming ATL-CR cells (Figure 3B). Immunofluorescence staining also demonstrated increased nuclear and cytoplasmic expression of MDR1 in MCA-forming ATL-CR cells, and coexpression of CD44 in some $MDR1^{+}$ cells (Figure 3C). Treatment with other HDAC inhibitors such as VPA and NaB also increased MDR1 expression in ATL-CR cells (Figure 3D), suggesting again that MDR1 expression may assist the survival of CD44 high CSC-like ATL cells. MDR1 expression is regulated by NF-κB signaling [34]. We therefore compared NF-κB activity between ATL-CR cells cultured

alone and ATL-CR cells cocultured with HEK293T cells, which revealed significantly increased NF-κB activity in cocultured ATL-CR cells (Figure 3E).

3.4. Blockade of NF-κB signaling inhibits Ad-MCA formation and the emergence of CD44 high CSC-like ATL cells

Next, we examined whether inhibition of NF-κB signaling affects MCA formation. When ATL-CR cells were cocultured with HEK293T cells in the presence of an NF-κB inhibitor, Bay 11-7082, the percentage of ATL cells adhering to HEK293T cells was markedly decreased compared to the control ($p<0.005$) (Figure 4A), and Ad-MCA formation by ATL cells was also strongly suppressed (Figure 4B). To examine whether Bay 11-7082 treatment can block NF-κB activity in ATL cells adhering to HEK293T cells, we performed reporter gene assays. As expected, the transcriptional activity of NF-κB was decreased by treatment with Bay 11-7082 (Figure 4C). However, a considerable number of ATL-CR cells still retained the ability to adhere to HEK293T cells even after treatment with high concentrations of Bay 11-7082 (Figure 4D). Similar results were obtained when ATL-CR cells were cocultured with 1C3IKEI cells (normal human epithelium-derived primary cells) (Figure 4E). Importantly, blockade of NF-κB signaling reduced expression of CD44, MDR1, and Nanog in adhering ATL-CR cells

(Figure 4F). Thus, NF-κB signaling is critically involved in Ad-MCA formation and the induction of CD44 high CSC-like ATL cells.

3.5. Disruption of vimentin structure prevents Ad-MCA formation by ATL cells

The majority of ATL-CR cells that retained adhesion to HEK293T cells after treatment with Bay 11-7082 exhibited the CD44 low/vimentin high phenotype (Figure 5A). Also, the cells with this phenotype were abundant in the outer border of the lower portion of MCAs attaching to the feeder layer (Figure 5B, arrowheads), suggesting that the cells at this location have a tendency not to express CD44. In addition, Jurkat cells, a $CD44^{-}$ T-cell lymphoma cell line, which adhered to HEK293T cells, but formed no MCA, strongly expressed vimentin in the presence or absence of Bay 11-7082 (Figure 5C, left panels). Jurkat cells also exhibited very low intrinsic NF-κB activity compared to ATL-CR cells, and this activity was not significantly increased by coculture (Figure 5C, right graph), consistent with the results that MCA formation requires enhanced NF-κB activity (Figure 4). Collectively, these observations suggested that vimentin might be involved in the adhesion of ATL cells to the feeder layer and anchor formation through an NF-κB-independent mechanism.

Withaferin A (WFA) is a vimentin inhibitor that binds to vimentin and alters its

distribution [30]. When ATL-CR cells cocultured with HEK293T cells were treated with WFA, the adhesion of ATL-CR cells to the feeder layer was markedly suppressed, and the size of Ad-MCAs was reduced in a dose-dependent manner (Figure 6A). Treatment with Bay 11-7082 or WFA did not induce appreciable apoptosis in ATL-CR cells cocultured with HEK293T cells, suggesting that inhibition of MCA formation is not the consequence of cell death (Figure 6B). In ATL-CR cells cultured alone, less than 20% of cells underwent apoptosis, suggesting that Bay 11-7082 and WFA exert limited cytotoxic effects even on ATL-CR cells cultured alone.

These observations were reproduced in primary ATL cells cultured on a layer of HEK293T cells (Figure 6C and D). WFA treatment disturbed the polarized orientation of vimentin intermediate filaments toward the core of Ad-MCAs (Figure 6C, arrowheads), reduced both adhesion and Ad-MCA formation, and eliminated CD44 high cells typically seen in Ad-MCA-forming primary ATL cells (Figure 6D, left panels). WFA treatment exerted similar effects on HuT-78 cells cultured on a layer of HEK293T cells (Figure 6E), indicating that the disruption of vimentin structure by WFA suppresses Ad-MCA formation by ATL and other T-cell lymphoma cells.

4. DISCUSSION

The present study has demonstrated that ATL cells can acquire intractable CSC-like phenotypes when they form Ad-MCAs on a layer of epithelial-like HEK293 feeder cells, (Figure 1). Inhibition of NF-κB signaling suppressed Ad-MCA formation and subsequent emergence of CD44 high CSC-like ATL cells (Figures 4), demonstrating the critical role of the NF-κB pathway in the induction of CSC-like ATL cells.

ATL cells adhering to a layer of HEK293T feeder cells showed enhanced expression of vimentin, a prometastatic protein, in an NF-κB-independent manner (Figures 5). Furthermore, the disruption of vimentin structure by WFA, a compound derived from a medicinal herb with anti-metastatic and -angiogenic activity [35-37], strongly reduced adhesion of ATL cells to a layer of HEK293T cells and MCA formation by ATL cells (Figure 6), suggesting the involvement of vimentin in the anchoring of ATL cells to the feeder layer. On the basis of these observations, we suggest that WFA might be useful as complementary medicine for preventing the expansion of CSC-like cells in ATL patients. This is not inconsistent with the recent proposal that vimentin intermediate filaments are a potential molecular target in cancer therapy [38, 39].

HDAC inhibitors have emerged as a new class of chemotherapeutic agents

against cancer [40, 41]. Vorinostat has been approved by the FDA for cutaneous T cell lymphoma [42]. However, monotherapeutic and combined-therapeutic clinical trials with such HDAC inhibitors have met with only limited success in most types of cancers [43, 44]. In the present study, activation of the NF-κB signaling pathway induced expression of MDR1 in MCA-forming ATL cells, rendering them resistant to HDAC inhibitors (Figure 3). Generally, efficacy of anti-cancer drugs is evaluated *in vitro* by direct cytocidal activity using a single-culture system. Our present study suggests that such drug evaluation is insufficient for tissue-infiltrating lymphoma cells that could acquire CSC-like phenotypes.

Anchorage-independent metastatic cells occur as single cells or MCAs [45]. Recent work indicates that MCA formation determines gene expression, proliferation, drug resistance, and immune escape *in vitro* in follicular lymphomas [46]. Secondary T-cell to T-cell synaptic interactions promote the differentiation and critical synaptic exchange of cytokines such as interferon-γ [47]. Thus, MCA formation and ensuing phenotypic changes likely represent key events required for understanding the nature of invasive lymphoma cells.

In conclusion, our work has demonstrated that ATL cells can acquire intractable CSC-like phenotypes by simple overnight coculture with epithelial-like feeder cells *ex*

vivo. Such phenotypic changes may occur in ATL cells that have invaded tissues in the human body. Therefore, it is desirable to develop therapeutic strategies separately for leukemic cells that have invaded tissues and those that remain in the circulation. Ad-MCA formation by ATL cells might mimic poorly understood critical events that occur in metastatic colonization *in vivo*. The HEK293T-coculture system should be useful for not only elucidating the nature of CSC niches and the molecular mechanisms underlying the emergence of CSCs, but also developing new therapeutic reagents against invasive T-cell lymphomas.

5. CONFLICT OF INTEREST

The authors declare no conflicts of interest.

6. ACKNOLEDGEMENTS

This work was supported by JSPS KAKENHI Grant Number 26460464 and the Centre for Research in Infectious Diseases, School of Medicine and Medical Science, University College Dublin, Ireland. We thank Drs. Shuichi Ota and Takanori Teshima for supplying us with samples of blood from an ATL patient.

7. REFERENCES

[1] B.J. Poiesz, F.W. Ruscetti, A.F. Gazdar, P.A. Bunn, J.D. Minna, R.C. Gallo, Detection and isolation of type C retrovirus particles from fresh and cultured lymphocytes of a patient with cutaneous T-cell lymphoma, Proc Natl Acad Sci U S A, 77 (1980) 7415-7419.

[2] A.L. Bittencourt, M.e.F. de Oliveira, Cutaneous manifestations associated with HTLV-1 infection, Int J Dermatol, 49 (2010) 1099-1110.

[3] K. Ohshima, Pathological features of diseases associated with human T-cell leukemia virus type I, Cancer Sci, 98 (2007) 772-778.

[4] R. Nasr, H. El Hajj, Y. Kfoury, H. de Thé, O. Hermine, A. Bazarbachi, Controversies in targeted therapy of adult T cell leukemia/lymphoma: ON target or OFF target effects?, Viruses, 3 (2011) 750-769.

[5] K. Tsukasaki, O. Hermine, A. Bazarbachi, L. Ratner, J.C. Ramos, W. Harrington, D. O'Mahony, J.E. Janik, A.L. Bittencourt, G.P. Taylor, K. Yamaguchi, A. Utsunomiya, K. Tobinai, T. Watanabe, Definition, prognostic factors, treatment, and response criteria of adult T-cell leukemia-lymphoma: a proposal from an international consensus meeting, J Clin Oncol, 27 (2009) 453-459.

[6] Y. Tsutsumi, J. Shimono, N. Miyashita, T. Teshima, No effect of humanized CCR monoclonal antibody (mogamulizumab) on treatment-resistant adult T cell leukemia with meningeal infiltration, Leuk Lymphoma, 55 (2014) 457-459.

[7] B.J. Huntly, D.G. Gilliland, Leukaemia stem cells and the evolution of cancer-stem-cell research, Nat Rev Cancer, 5 (2005) 311-321.

[8] S.A. Mani, W. Guo, M.J. Liao, E.N. Eaton, A. Ayyanan, A.Y. Zhou, M. Brooks, F. Reinhard, C.C. Zhang, M. Shipitsin, L.L. Campbell, K. Polyak, C. Brisken, J. Yang, R.A. Weinberg, The epithelial-mesenchymal transition generates cells with properties of stem cells, Cell, 133 (2008) 704-715.

[9] M. Zöller, CD44: can a cancer-initiating cell profit from an abundantly expressed molecule?, Nat Rev Cancer, 11 (2011) 254-267.

[10] Y.J. Su, H.M. Lai, Y.W. Chang, G.Y. Chen, J.L. Lee, Direct reprogramming of stem cell properties in colon cancer cells by CD44, EMBO J, 30 (2011) 3186-3199.

[11] T. Ishimoto, O. Nagano, T. Yae, M. Tamada, T. Motohara, H. Oshima, M. Oshima, T. Ikeda, R. Asaba, H. Yagi, T. Masuko, T. Shimizu, T. Ishikawa, K. Kai, E. Takahashi, Y. Imamura, Y. Baba, M. Ohmura, M. Suematsu, H. Baba, H. Saya, CD44 variant regulates redox status in cancer cells by stabilizing the xCT subunit of system xc(-) and thereby promotes tumor growth, Cancer Cell, 19 (2011) 387-400.

[12] H. Chagan-Yasutan, K. Tsukasaki, Y. Takahashi, S. Oguma, H. Harigae, N. Ishii, J. Zhang, M. Fukumoto, T. Hattori, Involvement of osteopontin and its signaling molecule CD44 in clinicopathological features of adult T cell leukemia, Leuk Res, 35 (2011) 1484-1490.

[13] M.A. Huber, N. Azoitei, B. Baumann, S. Grünert, A. Sommer, H. Pehamberger, N. Kraut, H. Beug, T. Wirth, NF-kappaB is essential for epithelial-mesenchymal transition and metastasis in a model of breast

cancer progression, J Clin Invest, 114 (2004) 569-581.
[14] L.Y. Bourguignon, K. Peyrollier, W. Xia, E. Gilad, Hyaluronan-CD44 interaction activates stem cell marker Nanog, Stat-3-mediated MDR1 gene expression, and ankyrin-regulated multidrug efflux in breast and ovarian tumor cells, J Biol Chem, 283 (2008) 17635-17651.
[15] K. Hinohara, S. Kobayashi, H. Kanauchi, S. Shimizu, K. Nishioka, E. Tsuji, K. Tada, K. Umezawa, M. Mori, T. Ogawa, J. Inoue, A. Tojo, N. Gotoh, ErbB receptor tyrosine kinase/NF-κB signaling controls mammosphere formation in human breast cancer, Proc Natl Acad Sci U S A, 109 (2012) 6584-6589.
[16] J. Zhou, H. Zhang, P. Gu, J. Bai, J.B. Margolick, Y. Zhang, NF-kappaB pathway inhibitors preferentially inhibit breast cancer stem-like cells, Breast Cancer Res Treat, 111 (2008) 419-427.
[17] N. Mori, M. Fujii, S. Ikeda, Y. Yamada, M. Tomonaga, D.W. Ballard, N. Yamamoto, Constitutive activation of NF-kappaB in primary adult T-cell leukemia cells, Blood, 93 (1999) 2360-2368.
[18] N. Hironaka, K. Mochida, N. Mori, M. Maeda, N. Yamamoto, S. Yamaoka, Tax-independent constitutive IkappaB kinase activation in adult T-cell leukemia cells, Neoplasia, 6 (2004) 266-278.
[19] T. Borovski, F. De Sousa E Melo, L. Vermeulen, J.P. Medema, Cancer stem cell niche: the place to be, Cancer Res, 71 (2011) 634-639.
[20] L. Li, W.B. Neaves, Normal stem cells and cancer stem cells: the niche matters, Cancer Res, 66 (2006) 4553-4557.
[21] M.A. Solis, Y.H. Chen, T.Y. Wong, V.Z. Bittencourt, Y.C. Lin, L.L. Huang, Hyaluronan regulates cell behavior: a potential niche matrix for stem cells, Biochem Res Int, 2012 (2012) 346972.
[22] K. Takahashi, K. Tanabe, M. Ohnuki, M. Narita, T. Ichisaka, K. Tomoda, S. Yamanaka, Induction of pluripotent stem cells from adult human fibroblasts by defined factors, Cell, 131 (2007) 861-872.
[23] P. Havasi, M. Nabioni, M. Soleimani, B. Bakhshandeh, K. Parivar, Mesenchymal stem cells as an appropriate feeder layer for prolonged in vitro culture of human induced pluripotent stem cells, Mol Biol Rep, 40 (2013) 3023-3031.
[24] O. Hovatta, M. Mikkola, K. Gertow, A.M. Strömberg, J. Inzunza, J. Hreinsson, B. Rozell, E. Blennow, M. Andäng, L. Ahrlund-Richter, A culture system using human foreskin fibroblasts as feeder cells allows production of human embryonic stem cells, Hum Reprod, 18 (2003) 1404-1409.
[25] K. Takahashi, M. Narita, M. Yokura, T. Ichisaka, S. Yamanaka, Human induced pluripotent stem cells on autologous feeders, PLoS One, 4 (2009) e8067.
[26] P. Catalina, R. Montes, G. Ligero, L. Sanchez, T. de la Cueva, C. Bueno, P.E. Leone, P. Menendez, Human ESCs predisposition to karyotypic instability: Is a matter of culture adaptation or differential vulnerability among hESC lines due to inherent properties?, Mol Cancer, 7 (2008) 76.
[27] J.S. Draper, K. Smith, P. Gokhale, H.D. Moore, E. Maltby, J. Johnson, L. Meisner, T.P. Zwaka, J.A. Thomson, P.W. Andrews, Recurrent gain of chromosomes 17q and 12 in cultured human embryonic stem cells, Nat Biotechnol, 22 (2004) 53-54.
[28] Y. Miyatake, A.L. Oliveira, M.A. Jarboui, S. Ota, U. Tomaru, T. Teshima, W.W. Hall, M. Kasahara,

Protective roles of epithelial cells in the survival of adult T-cell leukemia/lymphoma cells, Am J Pathol, 182 (2013) 1832-1842.

[29] E.A. Wayner, S.G. Gil, G.F. Murphy, M.S. Wilke, W.G. Carter, Epiligrin, a component of epithelial basement membranes, is an adhesive ligand for alpha 3 beta 1 positive T lymphocytes, J Cell Biol, 121 (1993) 1141-1152.

[30] B. Grin, S. Mahammad, T. Wedig, M.M. Cleland, L. Tsai, H. Herrmann, R.D. Goldman, Withaferin a alters intermediate filament organization, cell shape and behavior, PLoS One, 7 (2012) e39065.

[31] Y. Miyatake, H. Ikeda, A. Ishizu, T. Baba, T. Ichihashi, A. Suzuki, U. Tomaru, M. Kasahara, T. Yoshiki, Role of neuronal interferon-gamma in the development of myelopathy in rats infected with human T-cell leukemia virus type 1, Am J Pathol, 169 (2006) 189-199.

[32] C.A. Schneider, W.S. Rasband, K.W. Eliceiri, NIH Image to ImageJ: 25 years of image analysis, Nature methods, 9 (2012) 671-675.

[33] Z. Wang, E. Oron, B. Nelson, S. Razis, N. Ivanova, Distinct lineage specification roles for NANOG, OCT4, and SOX2 in human embryonic stem cells, Cell Stem Cell, 10 (2012) 440-454.

[34] M. Bentires-Alj, V. Barbu, M. Fillet, A. Chariot, B. Relic, N. Jacobs, J. Gielen, M.P. Merville, V. Bours, NF-kappaB transcription factor induces drug resistance through MDR1 expression in cancer cells, Oncogene, 22 (2003) 90-97.

[35] W. Vanden Berghe, L. Sabbe, M. Kaileh, G. Haegeman, K. Heyninck, Molecular insight in the multifunctional activities of Withaferin A, Biochem Pharmacol, 84 (2012) 1282-1291.

[36] Z. Yang, A. Garcia, S. Xu, D.R. Powell, P.M. Vertino, S. Singh, A.I. Marcus, Withania somnifera root extract inhibits mammary cancer metastasis and epithelial to mesenchymal transition, PLoS One, 8 (2013) e75069.

[37] P. Bargagna-Mohan, A. Hamza, Y.E. Kim, Y. Khuan Abby Ho, N. Mor-Vaknin, N. Wendschlag, J. Liu, R.M. Evans, D.M. Markovitz, C.G. Zhan, K.B. Kim, R. Mohan, The tumor inhibitor and antiangiogenic agent withaferin A targets the intermediate filament protein vimentin, Chem Biol, 14 (2007) 623-634.

[38] G. Lahat, Q.S. Zhu, K.L. Huang, S. Wang, S. Bolshakov, J. Liu, K. Torres, R.R. Langley, A.J. Lazar, M.C. Hung, D. Lev, Vimentin is a novel anti-cancer therapeutic target; insights from in vitro and in vivo mice xenograft studies, PLoS One, 5 (2010) e10105.

[39] A. Satelli, S. Li, Vimentin in cancer and its potential as a molecular target for cancer therapy, Cell Mol Life Sci, 68 (2011) 3033-3046.

[40] P.A. Marks, V.M. Richon, R.A. Rifkind, Histone deacetylase inhibitors: inducers of differentiation or apoptosis of transformed cells, J Natl Cancer Inst, 92 (2000) 1210-1216.

[41] A.C. West, R.W. Johnstone, New and emerging HDAC inhibitors for cancer treatment, J Clin Invest, 124 (2014) 30-39.

[42] B.S. Mann, J.R. Johnson, M.H. Cohen, R. Justice, R. Pazdur, FDA approval summary: vorinostat for

treatment of advanced primary cutaneous T-cell lymphoma, Oncologist, 12 (2007) 1247-1252.
[43] E.A. Olsen, Y.H. Kim, T.M. Kuzel, T.R. Pacheco, F.M. Foss, S. Parker, S.R. Frankel, C. Chen, J.L. Ricker, J.M. Arduino, M. Duvic, Phase IIb multicenter trial of vorinostat in patients with persistent, progressive, or treatment refractory cutaneous T-cell lymphoma, J Clin Oncol, 25 (2007) 3109-3115.
[44] R.L. Piekarz, R. Frye, H.M. Prince, M.H. Kirschbaum, J. Zain, S.L. Allen, E.S. Jaffe, A. Ling, M. Turner, C.J. Peer, W.D. Figg, S.M. Steinberg, S. Smith, D. Joske, I. Lewis, L. Hutchins, M. Craig, A.T. Fojo, J.J. Wright, S.E. Bates, Phase 2 trial of romidepsin in patients with peripheral T-cell lymphoma, Blood, 117 (2011) 5827-5834.
[45] L.G. Hudson, R. Zeineldin, M.S. Stack, Phenotypic plasticity of neoplastic ovarian epithelium: unique cadherin profiles in tumor progression, Clin Exp Metastasis, 25 (2008) 643-655.
[46] P. Gravelle, C. Jean, J. Familiades, E. Decaup, A. Blanc, C. Bezombes-Cagnac, C. Laurent, A. Savina, J.J. Fournié, G. Laurent, Cell growth in aggregates determines gene expression, proliferation, survival, chemoresistance, and sensitivity to immune effectors in follicular lymphoma, Am J Pathol, 184 (2014) 282-295.
[47] A. Gérard, O. Khan, P. Beemiller, E. Oswald, J. Hu, M. Matloubian, M.F. Krummel, Secondary T cell-T cell synaptic interactions drive the differentiation of protective CD8+ T cells, Nat Immunol, 14 (2013) 356-363.

FIGURE LEGENDS

Figure 1. Ad-MCA formation induces CD44 high CSC-like ATL cells. A: HEK293T-coculture system. ATL cells were cultured on a monolayer of epithelial-like HEK293T feeder cells. Upper, middle, and lower portions of MCAs are defined as in the figure. **B**: A mixture of CFSE- and CytoRed-labeled ATL cells were cocultured on a monolayer of HEK293T cells for 18 h. **C**: HEK293T cells did not express CD44. **D**: Expression of CD44 and vimentin in ATL-CR cells cultured alone or cocultured with HEK293T cells for 18 h. **E and F**: CD44 and vimentin expression. PBMCs derived from ATL patients were cocultured with HEK293T cells (**E**) or HuT-78 cells (**F**) for 18h. Images were captured by an Olympus DP70 camera. Bars represent 50 μm (**B and C**) and 25 μm (**D-F**).

Figure 2. ATL cells forming Ad-MCAs exhibit extracellular microvesicles and CSC markers. A: $CD44^+$ extracellular microvesicles in ATL cells forming Ad-MCAs on a monolayer of feeder cells. ATL cells in the upper portion of MCAs were strongly positive for CD44 and exhibited $CD44^+$ extracellular microvesicles. **B**: $CD44^+$ extracellular microvesicles in MCA-forming HuT-78 cells. **C-D**: Expression of Nanog (**C**) and Sox2 (**D**) in MCA-forming ATL cells. After 18 h of coculture with HEK293T cells, expression of CD44 and pluripotency markers was examined by

immunofluorescence staining. Percentage of ATL-CR cells with indicated markers was evaluated after coculture for 18 h (**D,** right graph). $CD44^+$ indicates the percentage of $CD44^+$ cells out of all MCA-forming ATL-CR cells. $CD44^+Sox2^+$ and $CD44^-Sox2^+$ represent percentages of $Sox2^+$ cells in $CD44^+$ and $CD44^-$ MCA-forming ATL-CR cells, respectively. Sox2-expresssing cells were counted for ~360 Ad-MCAs in 120 randomly selected high-power fields (×200). Arrowheads indicate ATL cells co-expressing CD44 and a pluripotent marker; arrows indicate pluripotent marker-positive, but CD44-negative ATL cells. Bars represent 10 μm (**A and B**) and 25 μm (**C and D**).

Figure 3. MDR1 expression is elevated on ATL cells forming Ad-MCAs. A: Cell cycle analysis in ATL-CR cells. ATL cells were cultured alone or cocultured with HEK293T cells in the presence of TSA for 24 h. HEK293T cells were labeled with CFSE 1 day before coculture. After coculture, non-adherent ATL-CR cells in the supernatant were separated from ATL-CR cells adhering to the monolayer of CFSE-labeled HEK293T cells. Cell cycle analysis was performed by FCM. Apo, apoptotic cells. **B-D**: Expression of MDR1. Cell surface expression of MDR1 on adhering and non-adhering ATL-CR cells by FCM (**B**). ATL-CR cells were cocultured with HEK293T cells for 18 h. Expression of CD44 and MDR1 in ATL-CR cells

cocultured with HEK293T cells for 18 h in the presence of 0.8 μM TSA (**C**), 1 mM NaB, or 0.2 mM VPA (**D**). **E**: NF-κB activity in ATL-CR cells. ATL-CR cells were cotransfected with 1 μg of NF-κB firefly luciferase reporter plasmids together with 50 ng of pRL-TK 1 day before coculture with HEK293T cells. After 18 h of coculture, reporter activities were measured and normalized to *Renilla* luciferase values. The values indicate mean fold-increases obtained by three independent experiments normalized to the untreated control sample. Error bars represent SD. ATL-CR sup, ATL-CR cells cultured with medium conditioned by HEK293T cells; cocultured ATL-CR, ATL-CR cells directly cocultured with HEK293T cells. Bars represent 50 μm.

Figure 4. Blockade of NF-κB signaling inhibits Ad-MCA formation and the emergence of CD44 high CSC-like ATL cells. A: Percentage of ATL-CR cells adhering to HEK293T cells after coculture for 18 h in the presence of 10 μM of Bay 11-7082. **B-C**: CFSE-labeled ATL-CR cells were cocultured with HEK293T cells in the presence or absence of 10 μM Bay 11-7082 for 18 h. Bay 11-7082 inhibits Ad-MCA formation by ATL-CR (**B**). Transcriptional activity of NF-κB in ATL-CR cells adhering to HEK293T cells (**C**). **D**: Bay 11-7082 does not eliminate adhesion of ATL-CR cells to the feeder layer. Percentage of ATL-CR cells adhering to HEK293T cells in a

microscopic field is shown in the graph on the right. The percentage of CFSE-labeled ATL-CR cells adhering to HEK293T cells was expressed as the proportion of $CFSE^+$ area within the total area in 20 randomly selected high-power fields (×200) using ImageJ 1.46. **E**: Bay 11-7082 inhibits Ad-MCA formation by 1C3IKEI cells. CFSE-labeled ATL-CR cells cocultured with 1C3IKEI cells in the presence or absence of 10 μM Bay 11-7082 for 18 h. **F**: Expression of CD44 and MDR1 in ATL-CR cells cocultured with HEK293T cells in the absence or presence of 10 μM Bay 11-7082 (left panels). Expression of Nanog, CD44, and vimentin in ATL-CR cells cocultured with HEK293T cells treated with 10 μM Bay 11-7082 (right panels). Error bars represent SD. **$p<0.01$. Bars represent 100 μm (**B, D** and **E**) and 50 μm (**F**). ImageJ 1.46 was used for image analysis (**D** and **E**).

Figure 5. CD44 low/vimentin high ATL cells adhere to the feeder layer in an NF-κB independent manner. **A**: Expression of CD44 and vimentin in ATL-CR cells in the presence or absence of 10 μM Bay 11-7082 for 18 h. **B:** CFSE-labeled ATL-CR cells adhering to HEK293T cells in the absence of 10 μM Bay 11-7082. **C**: Expression of CD44 and vimentin in Jurkat cells cultured alone or cocultured with HEK293T cells in the presence or absence of 10 μM Bay 11-7082 for 18 h (left panels). NF-κB activity

was compared with and without coculture in ATL-CR and Jurkat cells (graph on the right). Error bars represent SD. Bars represent 50 μm (**A , B,** left panels**, and C**) and 10 μm (**B,** right panels).

Figure 6. Disruption of vimentin structure prevents Ad-MCA formation by T-cell lymphoma cells. A: Expression of vimentin in CFSE-labeled ATL-CR cells cocultured with HEK293T cells in the presence or absence of 1 μM WFA for 18 h (left panels). The percentage of CFSE-labeled ATL-CR cells adhering to HEK293T cells was expressed as the proportion of $CFSE^+$ areas within the total area in 20 randomly selected high-power fields (×200) using ImageJ 1.46 (graph on the middle). Relative Ad-MCA size was expressed as the size of $CFSE^+$ area within each Ad-MCA in 20 randomly selected fields (graph on the right). **B**: Cell cycle analysis. ATL-CR cells were cultured alone or cocultured with HEK293T cells in the presence of WFA or Bay 11-7082 for 18 h. Cell cycle analysis was performed by FCM. Apo, apoptotic cells. **C and D**: Disruption of vimentin structure prevents Ad-MCA formation in PBMCs derived from an ATL patient. PBMCs derived from an ATL patient were cocultured with HEK293T cells with or without 0.5 μM of WFA, and then subjected to immunofluorescence staining for CD44 or vimentin. Expression of CD44 and vimentin in ATL cells adhering to HEK293T cells

(**C**). PBMCs cultured alone or cocultured with HEK293T cells with or without 0.5 μM of WFA or 10 μM of Bay 11-7082. Percentage of ATL-CR cells adhering to HEK293T cells in a microscopic field (**D**, graph on the right). The percentage of CD44-positive ATL-CR cells adhering to HEK293T cells was expressed as the proportion of $CD44^{+}$ areas within the total area in 10 randomly selected high-power fields (×200) using ImageJ 1.46. **E**: Disruption of vimentin structure prevents Ad-MCA formation in HuT-78 cells. HuT-78 cells were cultured alone or cocultured with HEK293T cells with or without 0.5 μM of WFA. The data are presented as the mean values of three independent experiments. Error bars represent SD. *$p<0.01$. Bars represent 50 μm (**A and D**), 25 μm (**C**) and 10 μm (**E**).

Figure 1

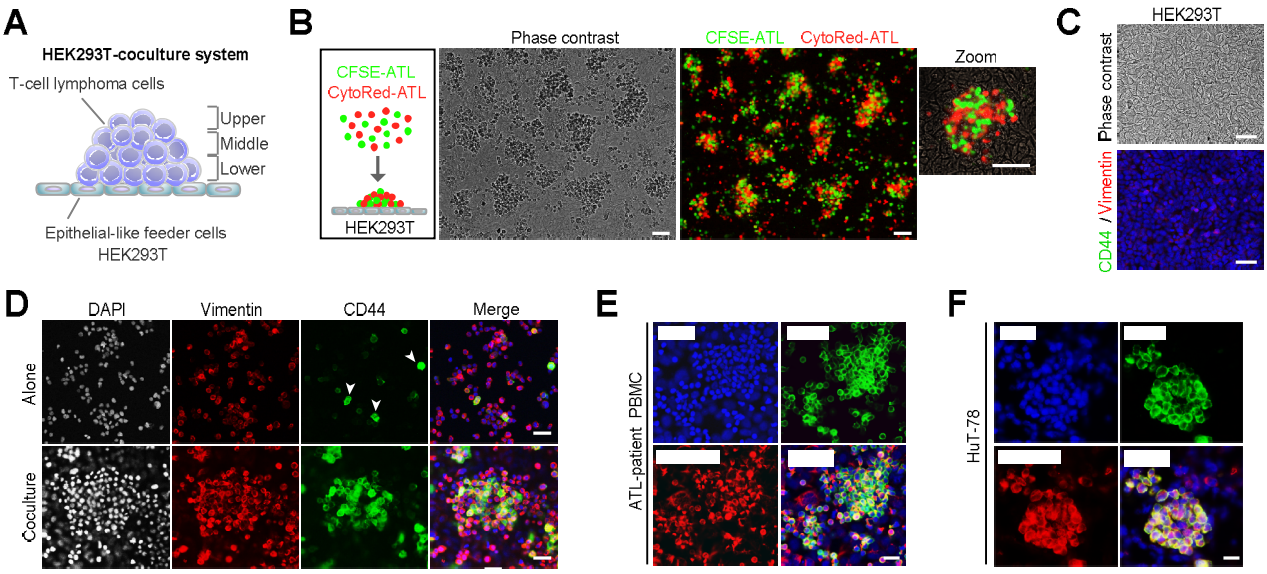
A
HEK293T-coculture system
T-cell lymphoma cells
Upper
Middle
Lower
Epithelial-like feeder cells
HEK293T
B
CFSE-ATL
CytoRed-ATL
HEK293T
Phase contrast
CFSE-ATL CytoRed-ATL
Zoom
C
HEK293T
Phase contrast
CD44 / Vimentin
D
DAPI
Vimentin
CD44
Merge
Alone
Coculture
E
ATL-patient PBMC
F
HuT-78

Figure 2

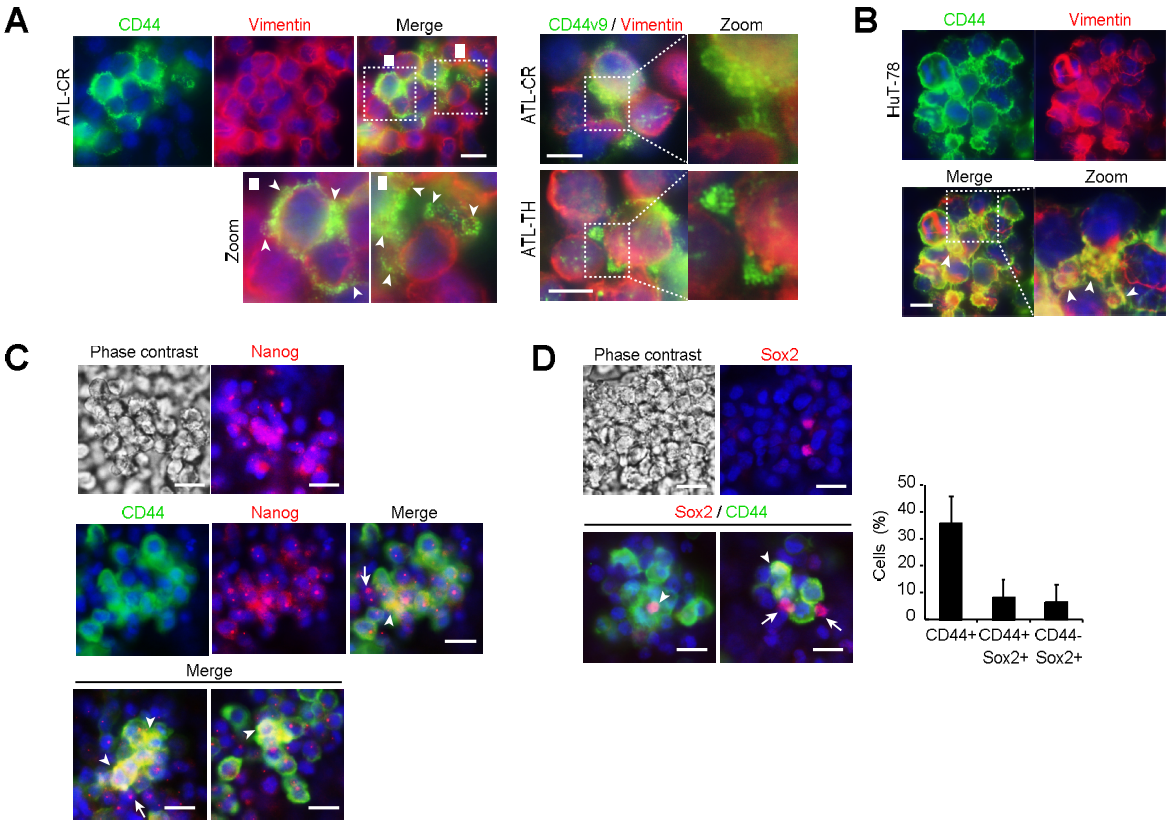
A
CD44
Vimentin
Merge
ATL-CR
Zoom
CD44v9 / Vimentin
Zoom
ATL-CR
ATL-TH
B
CD44
Vimentin
HuT-78
Merge
Zoom
C
Phase contrast
Nanog
CD44
Nanog
Merge
Merge
D
Phase contrast
Sox2
Sox2 / CD44
Cells (%)
50
40
30
20
10
0
CD44+ Sox2+
CD44+ Sox2+
CD44- Sox2+

Figure 3

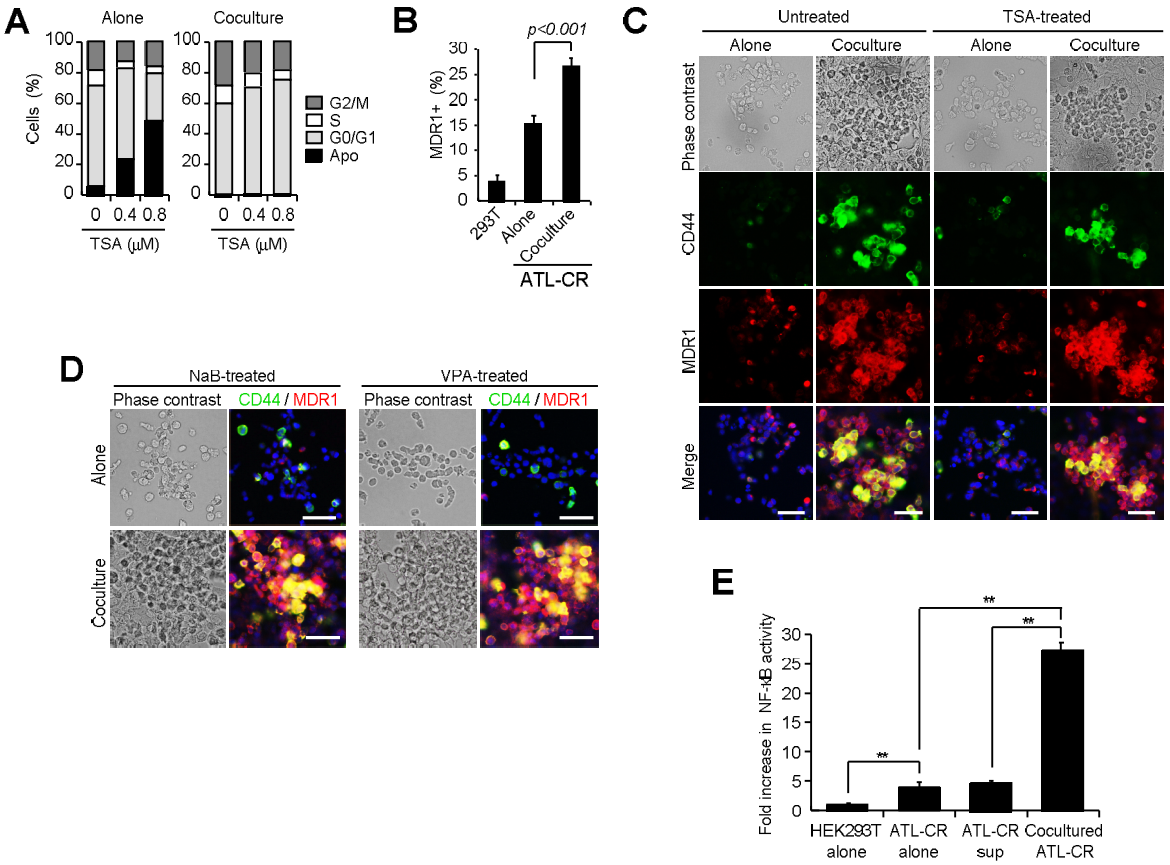
A
Alone
Coculture
Cells (%)
100
80
60
40
20
0
0 0.4 0.8
TSA (μM)
G2/M
S
G0/G1
Apo
B
p<0.001
MDR1+ (%)
30
25
20
15
10
5
0
293T
Alone
Coculture
ATL-CR
C
Untreated
TSA-treated
Alone
Coculture
Alone
Coculture
Phase contrast
CD44
MDR1
Merge
D
NaB-treated
VPA-treated
Phase contrast
CD44 / MDR1
Phase contrast
CD44 / MDR1
Alone
Coculture
E
Fold increase in NF-κB activity
30
25
20
15
10
5
0
**
**
**
HEK293T alone
ATL-CR alone
ATL-CR sup
Cocultured ATL-CR

Figure 4

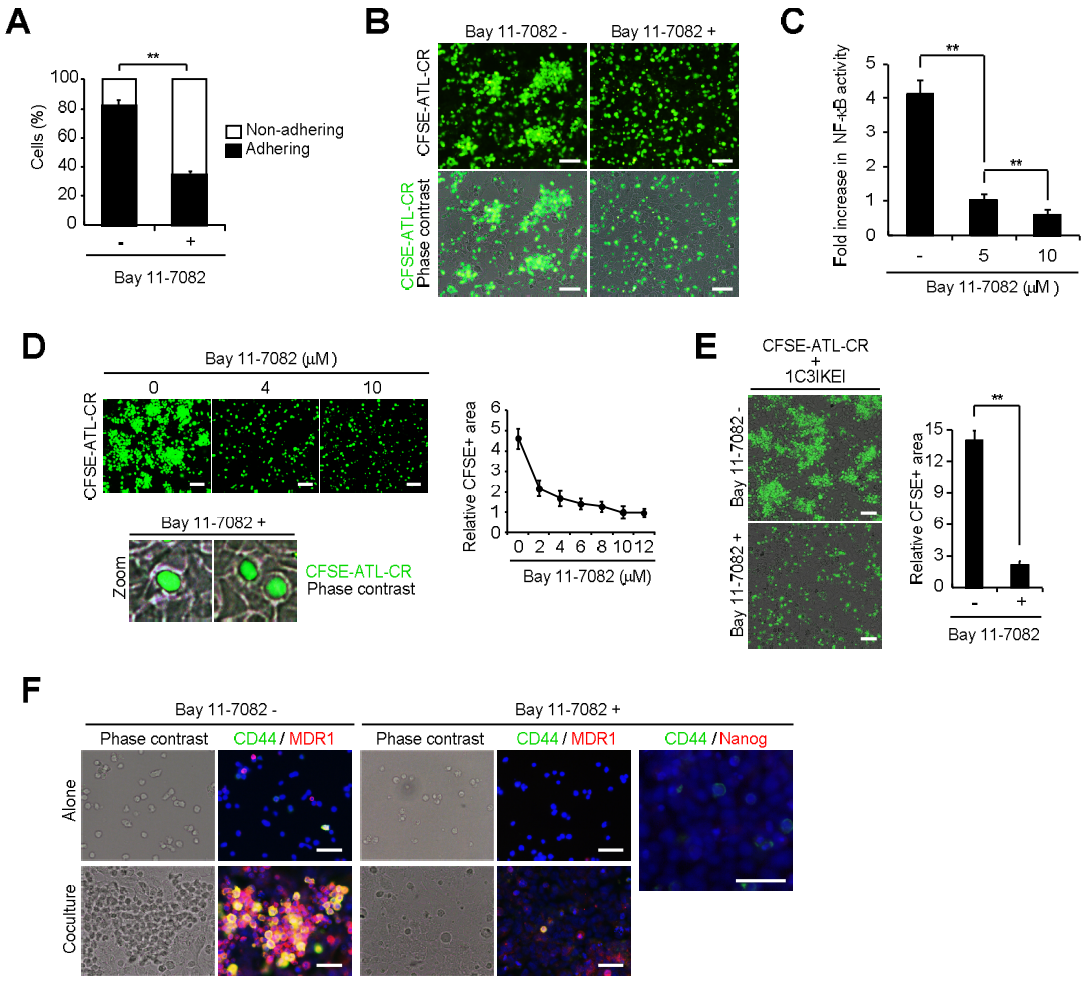
A
Cells (%)
Non-adhering
Adhering
Bay 11-7082
B
Bay 11-7082 -
Bay 11-7082 +
CFSE-ATL-CR
CFSE-ATL-CR
Phase contrast
C
Fold increase in NF-κB activity
Bay 11-7082 (μM)
D
Bay 11-7082 (μM)
CFSE-ATL-CR
Zoom
Relative CFSE+ area
E
CFSE-ATL-CR
+
1C3IKEI
Relative CFSE+ area
F
Phase contrast
CD44 / MDR1
CD44 / Nanog
Alone
Coculture

Figure 5

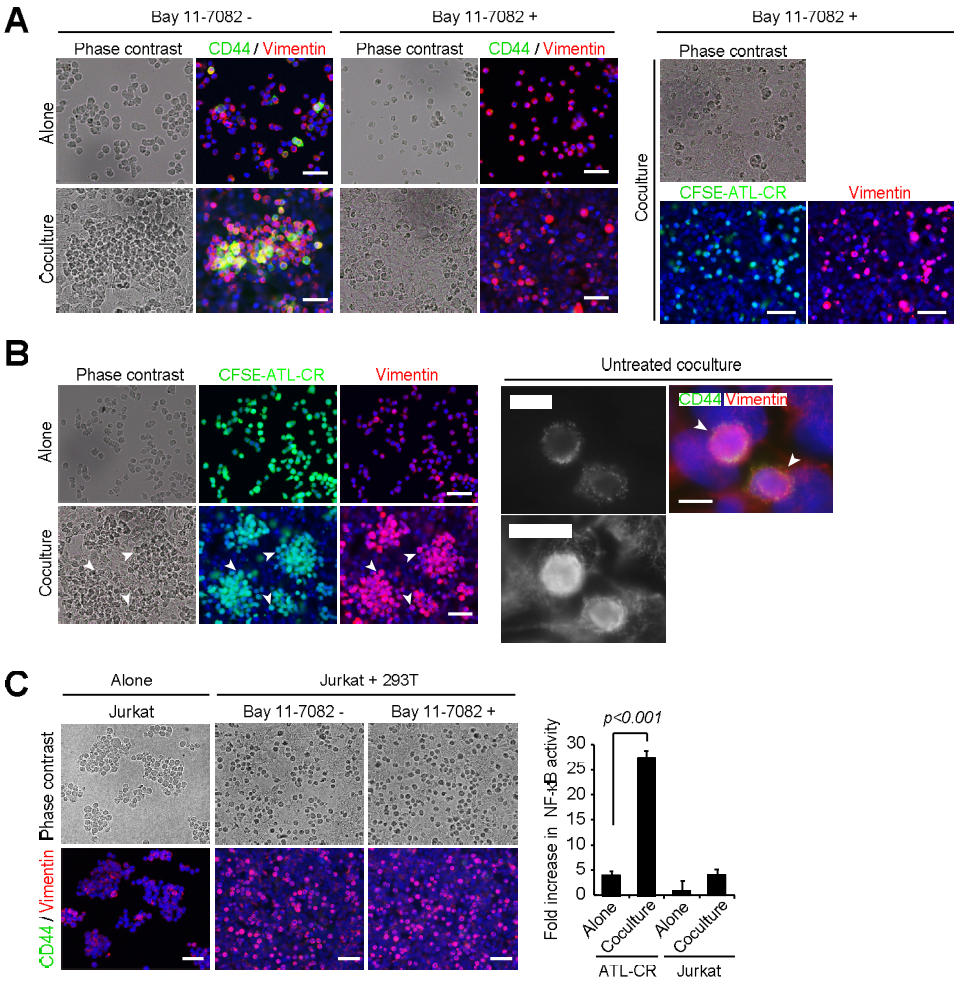
A
Bay 11-7082 -
Bay 11-7082 +
Bay 11-7082 +
Phase contrast
CD44 / Vimentin
Phase contrast
CD44 / Vimentin
Phase contrast
Alone
Coculture
Coculture
CFSE-ATL-CR
Vimentin
B
Phase contrast
CFSE-ATL-CR
Vimentin
Untreated coculture
Alone
Coculture
CD44 Vimentin
C
Alone
Jurkat + 293T
Jurkat
Bay 11-7082 -
Bay 11-7082 +
Phase contrast
CD44 / Vimentin
p<0.001
Fold increase in NF-κB activity
30
25
20
15
10
5
0
Alone
Coculture
Alone
Coculture
ATL-CR
Jurkat

Figure 6

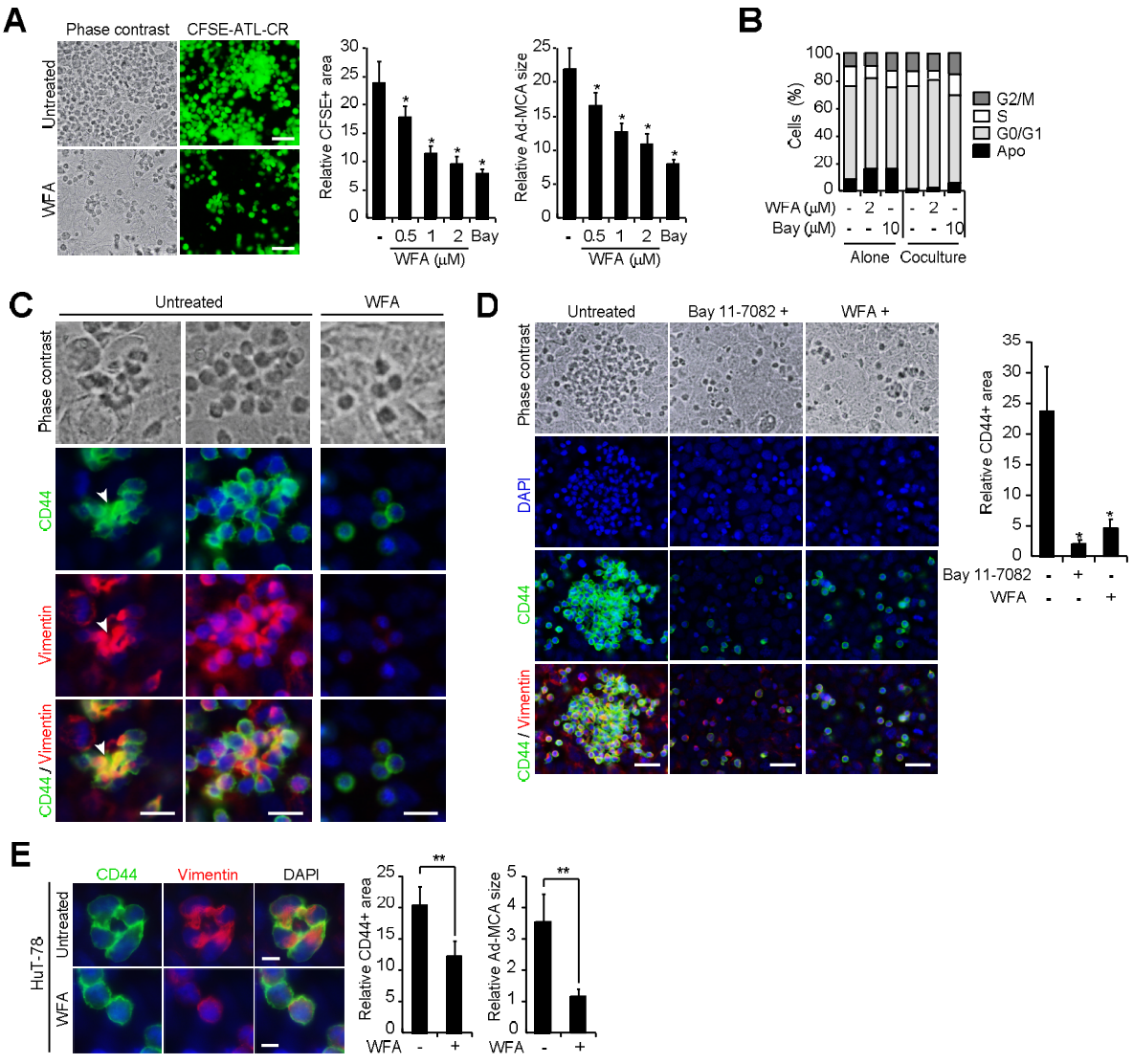
A
Phase contrast
CFSE-ATL-CR
Untreated
WFA
Relative CFSE+ area
Relative Ad-MCA size
- 0.5 1 2 Bay
WFA (μM)
B
Cells (%)
G2/M
S
G0/G1
Apo
WFA (μM) - 2 - - 2 -
Bay (μM) - - 10 - - 10
Alone
Coculture
C
Untreated
WFA
Phase contrast
CD44
Vimentin
CD44 / Vimentin
D
Untreated
Bay 11-7082 +
WFA +
Phase contrast
DAPI
CD44
CD44 / Vimentin
Relative CD44+ area
Bay 11-7082 - + -
WFA - - +
E
CD44
Vimentin
DAPI
HuT-78
Untreated
WFA
Relative CD44+ area
Relative Ad-MCA size
WFA - +